

## Fuel selection for a regenerative organic fuel cell/flow battery: thermodynamic considerations†

C. Moyses Araujo,<sup>bc</sup> Davide L. Simone,<sup>a</sup> Steven J. Konezny,<sup>bd</sup> Aaron Shim,<sup>b</sup> Robert H. Crabtree,<sup>bcd</sup> Grigori L. Soloveichik<sup>\*a</sup> and Victor S. Batista<sup>\*bcd</sup>

Received 3rd July 2012, Accepted 24th August 2012

DOI: 10.1039/c2ee22749e

Our work focuses on the feasibility of utilizing organic fuels for virtual hydrogen flow cell battery systems, based on thermodynamic considerations of fuel hydrogenation/dehydrogenation reactions. An assessment of the energy density and open circuit potentials (OCPs) as determined by the structure of carbocyclic and heterocyclic saturated hydrocarbons and their dehydrogenation products has been pursued and we identified promising organic carriers that could yield theoretical OCPs higher than that for the hydrogen fuel cell.

### Introduction

With growing interest in deployment of renewable intermittent energy sources, the need for electrical energy storage (EES) in both mobile and stationary applications is a key driver for exploratory research. Our goal is to increase the energy density of the EES system on both gravimetric and volumetric bases, while limiting our search to organic fuels containing elements that can be supplied on the needed global scale (C, H, N and O). Electrochemical energy storage technologies have several advantages compared to other options such as superconductive electromagnetic storage, flywheels, pumped hydro, and compressed air energy storage.<sup>1</sup> While lithium-ion batteries are considered to be a preferred battery

technology choice for mobile applications, redox flow batteries and sodium nickel chloride batteries are the least expensive and more suitable for stationary energy storage applications. Unlike secondary batteries, in redox flow batteries the energy capacity and the power are separated. The battery capacity is determined by the size of electrolyte tanks, while the power is determined by the size of the electrochemical cell thus allowing a flexible layout. Additional advantages of redox flow batteries are the ability to fully charge and discharge without damaging the cell, long life of the electrolytes, flexible operation, modular design, and moderate cost.<sup>2</sup> Major disadvantages of redox flow batteries are the extremely low energy storage density on a systems level, which is lower compared to even lead-acid batteries, and corrosion issues.<sup>3</sup>

Hydrogen, as the energy storage medium, is a clean, environmentally benign fuel that produces only water upon reaction with oxygen. Hydrogen in liquid or gaseous form has been proposed for long-term seasonal energy storage and for compensation of fluctuation of intermittent energy sources.<sup>4</sup> The storage of pressurized H<sub>2</sub> in underground caverns is most suitable for large-scale (>10 GWh) applications<sup>5</sup> and was demonstrated at the industrial scale by Praxair.<sup>6</sup>

The hydrogen fuel is used both in fuel cells as well as in combustion engines although it has relatively low volumetric

<sup>a</sup>GE Global Research, Niskayuna, New York 12309, USA. E-mail: soloveichik@ge.com; Fax: +1 518 387 7403; Tel: +1 518 3877906

<sup>b</sup>Yale University, Department of Chemistry, New Haven, CT 06520, USA. E-mail: victor.batista@yale.edu; carlos.araujo@yale.edu; Fax: +1 203 432 6144; Tel: +1 203 432 6672

<sup>c</sup>Yale Climate and Energy Institute, Yale University, P.O. Box 208109, New Haven, CT 06520-8109, USA

<sup>d</sup>Energy Sciences Institute, Yale University, P.O. Box 27394, West Haven, CT 06516-7394, USA

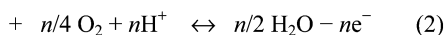
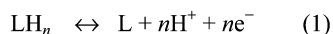
† Electronic supplementary information (ESI) available. See DOI: 10.1039/c2ee22749e

### Broader context

Recently, a novel concept of direct organic fuel cells based on 'virtual hydrogen' from reversible oxidative dehydrogenation of saturated organic compounds having a potential for developing safe high-density energy storage systems for mobile and stationary applications has been studied. The choice of organic fuels determines selection of other components (electrocatalyst and proton exchange membrane) for the proposed fuel cells. The main parameters of organic fuels for this purpose are energy density, fuel cell potential and efficiency, reversibility of dehydrogenation and hydrogenation reactions, safety and cost. The search for organic fuels with highest energy density stimulated the evaluation of saturated carbocyclic and heterocyclic hydrocarbons. These compounds with the highest hydrogen content and capable of dehydrogenating to form stable aromatic structures are promising candidates.

energy density (1.25 kW h L<sup>-1</sup>, when compressed at 690 bar and 15 °C, or 2.36 kW h L<sup>-1</sup> as a liquid), which is still higher than other EES options like advanced secondary batteries (0.15–0.65 kW h L<sup>-1</sup>), compressed air (0.017 kW h L<sup>-1</sup>) or pumped hydro (0.0004–0.0028 kW h L<sup>-1</sup>).<sup>7</sup> In contrast, the energy density of gasoline is 4–8 times higher (9.5 kW h L<sup>-1</sup>). Therefore, hydrogen storage in complex hydrides (*e.g.*, as lithium borohydride with 12.0 kW h L<sup>-1</sup>) or chemical hydrides (*e.g.*, as NH<sub>3</sub>BH<sub>3</sub>) represents an attractive higher energy density alternative (3.2–3.6 kW h L<sup>-1</sup>) but suffers from poor kinetics or low reversibility of hydrogen uptake/release.<sup>8</sup> Furthermore, the system requirements usually reduce the energy density by a factor of 2 or more.<sup>9</sup> Another possibility is hydrogen storage by hydrogenation of organic compounds, offering the possibility of using them with the existing fuel infrastructure.<sup>10</sup> Although these were suggested as hydrogen carriers about 25 years ago,<sup>11</sup> so far they have been explored mostly in the context of thermal dehydrogenation to produce hydrogen gas, which is fed to a conventional PEM hydrogen fuel cell.<sup>12</sup> However, hydrogen release requires an additional step employing high temperature and expensive noble metal catalysts.

In our ‘virtual hydrogen’ approach, the H<sub>2</sub> release step is replaced with the electrochemical step which releases protons and electrons while generating power. This alternative approach is based on electrochemical energy storage, where reversible partial electrochemical dehydrogenation of liquid organic fuels (eqn (1)) is combined with oxygen reduction at the cathode (eqn (2)), as recently proposed:<sup>10a,13</sup>



The conceptual ‘virtual hydrogen’ fuel cell/flow battery operates using two electrochemical reactions: (1) the anode reaction electrodehydrogenates LH<sub>*n*</sub>, a liquid organic hydrogen carrier (LOHC), to generate protons and electrons in the presence of an electrocatalyst (Fig. 1, blue arrow); (2) the protons that pass through the proton exchange membrane (PEM) react with O<sub>2</sub> at the cathode to generate water (Fig. 1, gray arrow).<sup>14</sup> The overall reaction (3) is thus the partial oxidation of the LOHC. In principle,

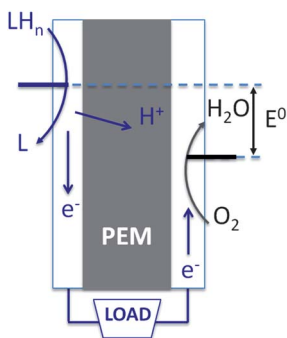
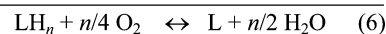
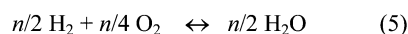
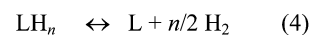


**Fig. 1** Fuel cell/flow battery based on dehydrogenation of liquid organic hydrogen carriers (LOHCs), LH<sub>*n*</sub>, giving an open circuit potential (OCP) E<sup>0</sup> relative to O<sub>2</sub> reduction.

all reactions are chemically reversible, which also allows the fuel cell to be used as an electrolyzer for hydrogenating L with protons from water and electrons from an electric power input. When acting in this way, the system is a flow battery in which the high energy hydrogenated fuel is stored separately from the electrochemical cell thus increasing the system’s energy density by an order of magnitude compared with what has been seen in prior flow batteries (75–140 W h kg<sup>-1</sup>)<sup>1</sup> keeping the system’s energy density comparable with direct methanol fuel cells. A few examples of successful electrochemical partial dehydrogenation of organic fuels have already been reported, such as with 2-propanol and with cyclohexane in the vapour phase.<sup>15</sup> Fuel cells utilizing low-temperature heat for hydrogenation of acetone using 2-propanol<sup>15c</sup> and hydrogen gas<sup>16</sup> as hydrogen source have been proposed. When compared to conventional hydrogen fuel-cell reactions,



a key advantage of the ‘virtual hydrogen’ scheme is that it avoids the release of hydrogen gas (eqn (4)), typically a strongly endothermic step, therefore by-passing the need for storage, transportation and safety issues associated with free hydrogen. In our case, we avoid this step and we expect the energy of dehydrogenation should therefore be minimized so as to increase the usable energy density of the organic carrier and thus position the dehydrogenation temperature in a reasonable range (at least below 180 °C).<sup>17</sup> This paper analyses potential fuels for virtual hydrogen flow cell/flow battery systems based on thermodynamic considerations of electrochemical hydrogenation/dehydrogenation reactions of organic compounds. Therefore, we focus on the energy analysis of reaction (3), which should be a good metric to identify promising fuels for virtual hydrogen storage, complementing earlier studies of thermal dehydrogenation, based on eqn (4).<sup>18</sup>

Cycloalkanes that can be reversibly dehydrogenated to stable aromatic compounds are good candidates for thermochemical energy conversion<sup>19</sup> and hydrogen storage.<sup>12</sup> Cyclohexane, with its high volumetric hydrogen density (56 g L<sup>-1</sup>) and low cost, was the first LOHC to be proposed.<sup>11</sup> However, the high volatility and toxicity of the dehydrogenation product, benzene, make the cyclohexane–benzene couple impractical. The methylcyclohexane–toluene couple has been suggested for seasonal energy storage but these LOHCs are also very volatile.<sup>20</sup> Decalin, which can be converted to naphthalene *via* a tetralin intermediate, is more convenient due to its low vapour pressure and the ability of the system to remain liquid even at high naphthalene concentrations.<sup>21</sup> Polycyclic aromatic hydrocarbons, either carbocyclic or with N or O heteroatoms, have also been suggested as dehydrogenated LOHCs.<sup>22</sup>

Pez *et al.*<sup>23</sup> have proposed *N*-alkylated carbazoles as LOHCs. In contrast to the parent solid carbazole, they are liquids or low melting solids, and *N*-ethylcarbazole can be reversibly hydrogenated to a fully saturated product, *N*-ethyl-dodecahydrocarbazole, with high rate and a selectivity of 98% using 5 wt% ruthenium on an alumina catalyst.<sup>24</sup> The saturated heterocyclic compound can also be effectively dehydrogenated by a homogeneous Ir pincer

complex<sup>25</sup> or over a supported Pd catalyst.<sup>26</sup> Substituted thiophenes, such as 2-methylthiophene, have been proposed as LOHCs because of the additional capacity associated with their ring opening (three molecules of H<sub>2</sub> per thiophene molecule),<sup>27</sup> but the possibility of hydrodesulfurization during the hydrogenation step limits their usefulness.

A severe problem that limits progress in the field is the scarcity of experimental thermodynamic parameters for promising LOHCs in the condensed state, especially in the case of non-aromatic compounds. For hypothetical materials, or ones that are not easily available, these data are practically impossible to obtain. There are some empirical methods like Benson's group additivity approach that can give satisfactory results but its applicability is limited to compounds that resemble the ones used to establish them in terms of their functional groups,<sup>28</sup> or the volume-based approach.<sup>29</sup> Vatani *et al.* accurately predicted the enthalpy of formation of different organic compounds using a genetic algorithm-based multivariate linear regression ( $R^2 = 0.983$ ).<sup>30</sup>

First-principles calculations based on density functional theory (DFT) have been employed to evaluate the thermodynamics of the dehydrogenation reactions of azaheterocycles.<sup>18,31</sup> Studies based on hybrid functionals (*e.g.*, B3LYP) and modest basis sets (*e.g.*, 6-311 + G(d,p)) showed that the placement of nitrogen atoms in cyclic molecules substantially reduces the heat of dehydrogenation, and the value of reduction correlates with a number of nitrogen atoms in the cycle.<sup>18</sup> It was demonstrated that the dehydrogenation enthalpy linearly depends on the Hammett  $\sigma$  (*para*) parameter for monosubstituted cyclohexanes and *para*-substituted piperidines, where the electron-donating groups in the side chain reduce the enthalpy.<sup>17</sup> The presence of conjugated substituents in cyclohexanes decreases the dehydrogenation enthalpy even more, though the linear dependence on the Hammett  $\sigma_{para}$  parameter remains.<sup>17</sup> Also, the values calculated for the enthalpy of dehydrogenation ( $\Delta H_d$ ) at the B3PW91/aug-cc-pVDZ level of theory were in excellent agreement with the experimental values for nine available single ring compounds ( $R^2 = 0.9985$ ).<sup>31</sup> The calculated thermodynamic values ( $\Delta H_d$ ,  $\Delta S_d$ , and  $\Delta C_v$ ) were used to obtain the dissociation temperature  $T_d$  which was shown to vary from 46 K for 2-methyl-2H-1,2,3-triazole to 980 K for cyclohexane.<sup>31</sup> These earlier theoretical studies of dehydrogenation are complemented by the results presented in this paper, which are focused on the standard fuel cell potentials of promising LOHCs, as determined by the thermodynamics of the electrochemical reaction (3). At the same time, the study provides benchmarks on the ability of DFT free energy calculations to correlate with measurements of electrochemical cell potentials.

## Methods

### Thermodynamic analysis

Standard cell potentials (open circuit potentials,  $E^0$ ) were computed from the overall reaction (3) free energy change  $\Delta G_r$ , as follows:

$$E^0 = -\Delta G_r/nF \quad (7)$$

where

$$\Delta G_r = G_L + n/2 G_{H_2O} - G_{LH_n} - n/4 G_{O_2} \quad (8)$$

with the *ab initio* molecular free energies of reactants and products in the gas phase, which is obtained as follows:

$$G = H - T(S_{\text{vib}} + S_{\text{rot}} + S_{\text{trans}}) \quad (9)$$

where

$$H = E_{\text{elect}} + U_{\text{vib}} + U_{\text{trans}} + U_{\text{rot}} + PV \quad (10)$$

with  $E_{\text{elect}}$  being the SCF total energy,  $U_{\text{vib}}$  the thermal vibrational energy computed from *ab initio* frequencies,  $U_{\text{trans}} = 3/2 k_B T$ ,  $U_{\text{rot}} = 3/2 k_B T$  and  $PV = k_B T$ . To reduce systematic errors, we define  $G_{O_2}$  in eqn (8) to match the experimental value of the free energy change of the reaction  $H_2O \rightarrow 1/2 O_2 + H_2$ , which is +237 kJ mol<sup>-1</sup> (water) or 2.46 eV.<sup>32</sup> The experimental free energy of hydration for water was also added.<sup>33</sup> Quantum chemistry calculations were carried out by using the software packages Spartan 08<sup>34</sup> and Gaussian 09.<sup>35</sup> *Ab initio* total energies and frequencies were calculated at the DFT B3LYP<sup>36</sup> level with the cc-PVTZ basis set<sup>37</sup> for fully optimized molecular configurations obtained at the same level without any symmetry constraint.

For comparison to experimental values, we compute the corresponding experimental free energy changes, as follows:

$$G = H - TS \quad (11)$$

with

$$H = H^0 + C_p(T - 298.15 \text{ K}) \quad (11a)$$

and

$$S = S^0 + C_p \ln(T/298.15 \text{ K}), \quad (11b)$$

which were computed from calorimetry data for standard enthalpies  $H^0$  and entropies  $S^0$  of reactants and products. All values used for standard enthalpies  $H^0$  and entropies  $S^0$  of reactants and products were taken from the NIST database<sup>38</sup> and the compilation by Ali<sup>39</sup> (Table S4 in the ESI†). For the range of potentials of interest (0.8–1.3 V), experimental errors in the free energy of reaction in the 10 kJ mol<sup>-1</sup> range result in a difference of cell potentials of about 50 mV.

### Calorimetric measurements

Calorimetric measurements for selected organic fuels were made to determine accuracy of the method by comparison with literature data.<sup>38,39</sup> Calorimetry of *N*-ethyl-dodecahydrocarbazole was measured to validate the developed correlation between experimental and computed OCPs. The commercially available studied compounds were purchased from Aldrich Chemical Co. with a purity  $\geq 99\%$  and used as received. *N*-Ethyl-dodecahydro-1*H*-carbazole was synthesized by hydrogenation of *N*-ethyl-9*H*-carbazole in heptane (1000 psi H<sub>2</sub>, 150 °C) in the presence of 5% ruthenium on a carbon catalyst according to the literature method.<sup>24a</sup> The resulting mixture contained six isomers (three pairs of diastereomers) of *N*-ethyl-dodecahydro-1*H*-carbazole and traces of unreacted starting material and partially hydrogenated compound (9-ethyl-2,3,4,5,6,7,8,9-octahydro-1*H*-carbazole). One of the diastereomers of *N*-ethyl-dodecahydro-1*H*-carbazole

was isolated by column chromatography with the configuration 4aS,4bS,8aS,9aR<sup>24a</sup> as determined by 2D NMR methods.

Calorimetric values for organic fuels were obtained from experiments using an IKA C200 calorimeter in conjunction with the ASTM D4809-00 standard.<sup>40</sup> Experimental data on combustion enthalpies and entropies of selected organic compounds are given in the ESI (Table S3†).<sup>38,39</sup> Dehydrogenation enthalpy and entropy changes for organic fuel pairs were calculated as usual, using Hess' Law.

## Results and discussion

### Thermodynamic analysis of organic fuel cells

Dehydrogenation of saturated organic molecules is endoergic. Making the process less endoergic (*e.g.*, by stabilization of dehydrogenation products *via* aromatization or conjugation effects) is desirable since the dehydrogenation energy acts as a penalty on the maximum achievable organic fuel cell potential compared to the hydrogen/oxygen fuel cell (1.23 V at 25 °C).

Values of the thermodynamic open-circuit potentials (OCPs)  $E^0$  at a standard temperature (25 °C) for known fuel/hydrogen-depleted fuel couples with tabulated thermodynamic parameters are given in Table 1. The OCP of organic fuel cells is higher when the dehydrogenation energy is lower. The smallest OCP is found when the dehydrogenation product has a triple carbon-carbon bond. Interestingly, if the dehydrogenation product is a compound with a triple carbon-nitrogen bond, the OCP is reasonably high (1.02 V for the *n*-propylamine/propionitrile couple; Table 1).

All known hydrogen-rich/hydrogen-depleted couples can be divided into two main groups in which the dehydrogenated product is either an unconjugated/conjugated alkene or an aromatic compound. When the product of dehydrogenation is an alkene, the standard cell potential is 350–400 mV lower than that of the hydrogen based fuel cell, even when the alkene is conjugated. However, for the second group, in which aromatic dehydrogenated products are formed, the cell potential drop relative to the hydrogen fuel cell is only about 110–170 mV, which is due to the aromatic stabilization (Table 1). Introducing nitrogen atoms into the ring slightly increases the cell potential by about 30 mV per nitrogen atom. The highest OCP is registered for the oxidation of the cyclohexadienes to the corresponding aromatic structures. These OCPs are even higher than the hydrogen/oxygen fuel cell OCP because the dehydrogenation in these cases is an exoergic process. Reasonably high OCPs are also calculated for partial dehydrogenation of secondary alcohols to ketones (~1.11 V) and amines to nitriles (Table 1).

The OCP for five-membered ring organic carriers C<sub>4</sub>H<sub>8</sub>X, dehydrogenated to aromatic structures, increases in the order of X = S ~ O < NH and is substantially higher than the case in which two conjugated double C=C bonds are formed (X = CH<sub>2</sub>,  $E^0 = 0.86$  V). In general, a nitrogen atom in the heterocyclic structure or in a side chain increases the OCP by about 30 mV per nitrogen atom.

Increasing the operating temperature of the hydrogen fuel cell decreases the OCP when both liquid and vaporized water are produced due to the entropy term. The OCP changes at points of reactant phase transformation from liquid to gas. One should

**Table 1** Free energy of dehydrogenation  $\Delta G$  and open circuit potential  $E^0$  for organic hydrogen carriers at 298 K

Fuel	Dehydrogenation product	$\Delta G$ , kJ mol <sup>-1</sup>	$E^0$ , V
Ethylbenzene	Phenylacetylene	-245.4	0.636
Ethylbenzene	Styrene	-155.9	0.808
Cyclooctane	Cyclooctatetraene	-667.7	0.821
Cyclohexane	Cyclohexene	-161.2	0.844
Cyclohexane	Cyclohexadiene	-322.5	0.836
Cyclopentane	Cyclopentene	-165.2	0.844
Cyclopentane	Cyclopentadiene	-329.5	0.853
Indane	1 <i>H</i> -Indene	-170.4	0.883
Cycloheptane	Cycloheptatriene	-520.0	0.889
Tetrahydrofuran	Furan	-390.4	1.011
Tetrahydro-thiophene	Thiophene	-390.6	1.012
2,3-Dihydro-benzofuran	Benzofuran	-207.9	1.077
<i>n</i> -Propylamine	Propionitrile	-395.1	1.024
Chloro-cyclohexane	Chlorobenzene	-596.7	1.031
Cyclohexane	Benzene	-613.9	1.061
Cyclohexanethiol	Thiophenol	-614.2	1.061
Methylcyclohexane	Toluene	-618.1	1.068
Cyclohexanol	Phenol	-623.6	1.077
<i>N</i> -Methylpyrrolidine	<i>N</i> -Methylpyrrole	-549.6	1.082
<i>cis</i> -Decalin	Naphthalene	-1240.9	1.086
Tetralin	Naphthalene	-419.2	1.086
Tetrahydro-quinoline	Quinoline	-421.5	1.092
Piperidine	Pyridine	-632.4	1.092
Cyclohexylamine	Aniline	-634.4	1.096
2-Methylpiperidine	2-Methylpyridine	-639.3	1.104
Isopropanol	Acetone	-213.2	1.105
2-Butanol	2-Butanone	-214.5	1.112
Piperazine	Pyrazine	-646.8	1.117
Pyrrolidine	Pyrrole	-433.7	1.124
1,4-Cyclohexadiene	Benzene	-288.5	1.495
1,3-Cyclohexadiene	Benzene	-291.4	1.510

note that the number of line breaks in the plot of Fig. 2 changes from one (both the fuel and product remain liquid) to two (one of them has phase change) to three (both the fuel and product undergo the phase change, *e.g.* the piperidine-pyridine couple). The slope of the OCP temperature dependence for gaseous products is smaller because the differences in entropy for a gas are higher than that for a liquid, as is observed for water above 100 °C. Though the cell potentials are lower for fuel cells based on dehydrogenation of heterocyclic fuels, the temperature slope above 100 °C becomes positive for the organic fuels, as shown in Fig. 2. For at least one fuel (piperazine) the potential reaches the potential of the hydrogen fuel cell at 150 °C. It is therefore shown

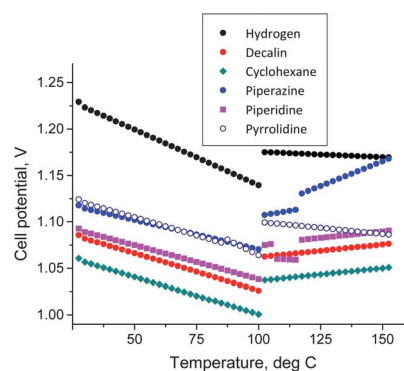


**Fig. 2** Temperature dependence of the OCP for organic fuels.

that increasing the operating temperature for a liquid organic fuel cell/flow battery would be beneficial in achieving high OCPs. Worth noting, the long-term stability of currently used PEMs above 90 °C remains a challenge and requires development of robust high temperature PEMs.

Table 2 shows that the specific energies of selected organic fuels are in the 1660–2095 W h kg<sup>-1</sup> range (material only), when assuming full dehydrogenation into aromatic products. Due to the low fuel density, however, the energy densities are in the 1350–1875 W h L<sup>-1</sup> range, except for the denser piperazine ( $\rho = 1.1 \text{ g cm}^{-3}$ ), which has a higher (2260 W h L<sup>-1</sup>) energy density. Though the specific energy of methanol (the standard liquid fuel for fuel cells) is much higher ( $\sim 6070 \text{ W h kg}^{-1}$ , assuming full oxidation), the need to work with diluted aqueous solutions (2 M concentration is optimal)<sup>41</sup> to prevent the fuel crossover effectively decreases this value to  $\sim 400 \text{ W h kg}^{-1}$  (or  $\sim 400 \text{ W h L}^{-1}$ ). Another drawback of direct methanol fuel cells (DMFCs) is low power density compared to hydrogen fuel cells.<sup>42</sup> In the proposed organic fuel cell/flow battery, an organic fuel is intended to be used as a neat liquid or as a concentrated mixture with the product of dehydrogenation thus making the system energy density much closer to the energy density of materials compared with DMFC or secondary batteries. This feature significantly increases attractiveness of organic fuels, with potential energy densities of about 4–5 times higher than that of direct methanol fuel cells. Assuming that the power density of the proposed direct organic rechargeable fuel cell is comparable with other direct liquid fuel cells, this energy storage system could be most suitable for large-scale EES. However, if effective electrocatalysts capable of providing high power density is designed, the proposed system may be applicable also for mobile applications, which are currently based on compressed (70 MPa) hydrogen.

Another important parameter for fuel cells is the theoretical maximum efficiency  $\eta = \Delta G/\Delta H$ .<sup>43</sup> For the hydrogen fuel cell the theoretical efficiency at 25 °C is 83%, which leads to a practical cell efficiency of about 50%, due to cathodic and anodic overpotentials and Ohmic losses. For organic fuels,  $\eta = 93\text{--}95\%$  at 25 °C (Table 2).

**Table 2** Boiling point, specific energy and energy density of selected organic fuels, and theoretical efficiency of fuel cells based on dehydrogenation

Organic carrier (in the hydrogenated state)	Boiling point, °C	Specific energy, W h kg <sup>-1</sup>	Energy density, W h L <sup>-1</sup>	Efficiency, %
Liquid hydrogen	-252.9	—	2539	83.0
Pyrrolidine	87	1660	1438	92.8
Tetrahydrofuran	66	1500	1334	93.4
Tetrahydrothiophene	119	1196	1195	93.5
Cyclohexane	80.7	2025	1578	94.1
Methylcyclohexane	101	1747	1345	94.3
Cyclohexylamine	134.5	1772	1532	95.2
Chlorocyclohexane	66	1403	1403	93.4
Cyclohexanol	160.8	1686	1622	93.0
Cyclohexanethiol	158	1292	1227	94.0
Piperidine	106	2046	1764	94.2
2-Methylpiperidine	118	1776	1499	94.5
Piperazine	146	2055	2260	95.7
<i>trans</i> -Decalin	187	2095	1877	93.1

## Correlation between theoretical and experimental $E^0$

The thermodynamic data needed to determine the theoretical OCP and energy density are available only for a limited number of fuel/dehydrogenated-fuel couples. Therefore, theoretical predictions are highly desirable. Here, we use first-principles methods to calculate organic carrier free energies (in hydrogenated and depleted forms) and obtain OCPs that can be directly compared to thermodynamic data (Fig. 3). The predictive power of Hartree–Fock, DFT, and Møller–Plesset (MP) methods has been compared in terms of  $R^2$ , coefficients for the resulting correlations of calculated and experimental data, obtaining MP/cc-pVTZ ( $R^2 = 0.780$ ) < HF/6-311 + G\*\* ( $R^2 = 0.961$ ) < MP/6-311++G\*\* ( $R^2 = 0.987$ ) < DFT/B3LYP/6-311++G\*\* ( $R^2 = 0.993$ ) < DFT/B3LYP/cc-pVTZ ( $R^2 = 0.994$ ). Note that while MP methods have been successfully applied for calculations of heats of formation for thousands of organic molecules,<sup>44</sup> the MP/cc-pVTZ gives the lowest correlation between calculated and experimental data of OCPs while DFT methods outperform the more time-consuming MP methods probably due to the inclusion of correlation beyond the perturbation theory level. It is worth noting that Spartan 08 and Gaussian 09 software packages delivered almost identical total energy values with standard deviation less than 0.1 kcal mol<sup>-1</sup> (see the ESI, Table S5†). Based on these results, further analysis has been carried out at the DFT B3LYP/cc-pVTZ level using the Gaussian 09 including thermochemical corrections according to eqn (9) (see Tables S6 and S7† for details). Fig. 3 shows the resulting correlation between experimental and calculated OCPs. The slope and intercept coefficients are 1.085 and -0.008, respectively, as determined by ordinary least square (OLS) regression, with  $R^2 = 0.994$  and the mean unsigned error (MUE) of 11.8 mV. The correlation shown in Fig. 3 has been further evaluated in terms of the experimental combustion enthalpy of *N*-ethyl-dodecahydro-1*H*-carbazole and *N*-ethyl-9*H*-carbazole. We obtain  $E^0 = 1.18 \pm 0.01 \text{ V}$  (ESI file, Table S3†), in a good agreement with the value predicted from computation of the main isomer (4*aR*,4*bS*,8*aS*,9*aS*)-9-ethyl-dodecahydro-1*H*-carbazole, namely 1.17 V (penultimate molecule in Table 6). We have also noted that using experimental data for determining the enthalpy of pyrrolidine (see Table S3† in the ESI file), instead of the literature value,<sup>38</sup> improves the correlation ( $R^2$ ) by 0.001 and decreases the MUE by 0.8 mV for all methods.

Note that we observed excellent correlation between experimental thermodynamic data for condensed phase and DFT calculation of single molecules in the gas phase, indicating that solvation energy and configurational entropy play a minor role. We have added solvation contribution to the OCP of cyclohexane–benzene fuel pair and found a potential energy change of only 7 mV. Details of this calculation are described in the ESI file.†

## Computational screening of heterocyclic LOHCs

Screening of LOHCs that form aromatic structures upon dehydrogenation has been performed at the B3LYP/cc-pVTZ level of theory, in conjunction with the linear correlation model of Fig. 3. Tables 3–6 summarize our results for a wide range of LOHCs, indicated in the table in their dehydrogenated states, including

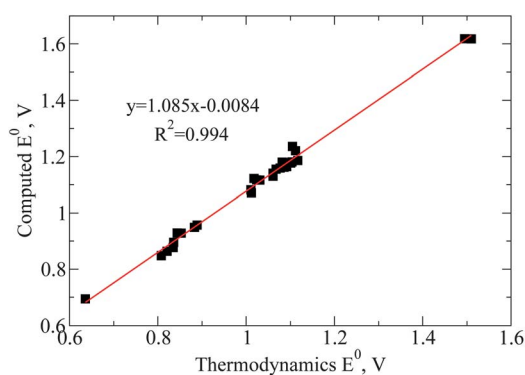


**Fig. 3** Correlation between OCPs obtained from the calculated free energies at the B3LYP/cc-PVTZ theory level and from the experimental thermodynamic data (NIST database) for different organic fuels.

theoretical OCPs for the resulting fuel cells based on the dehydrogenation reactions, and corresponding hydrogen gravimetric densities. Molecules have been selected to represent different ring types A–F, as illustrated in Fig. 4, including single and fused five- and six-membered rings and different heteroatoms (O, N and S). We have also calculated the free energy and theoretical OCPs for several *N*-alkylated fuels to compare with their non-substituted counterparts as well as for cyclohexanes and piperidines with donor and electron withdrawing substituents in the side chain. The motivation for such analysis has been that alkyl substituents typically expand the temperature range for the liquid state of aromatic molecules. For example, carbazole is a solid with a high melting point (245 °C) while *N*-ethylcarbazole has a much lower melting point (66 °C) and may be used at slightly elevated temperatures. Since mixtures with dodecahydro-*N*-ethylcarbazole stereoisomers have a melting point < –40 °C, they can be used at ambient conditions.<sup>45</sup>

Our particular interest in aromatic structures has been that the OCP is usually higher (>1.06 V) when an aromatic ring forms upon dehydrogenation of the LOHC. In contrast, compounds that do not form aromatic products (e.g. 4*H*-quinolizine and 1,4-dihydropentalene) have lower OCPs (<1.0 V).

Table 3 shows the estimated OCPs for structure types A and C. We show that introducing heteroatoms into the aromatic structures has significant effects on the resulting OCPs. For example, for six-membered rings (structure type A), introducing a N atom in the heterocyclic structure increases the OCP by 30–40 mV relative to the carbocyclic analogue. Addition of a second N atom further increases the OCP by ~30 mV. The third N in 1,3,5-triazine substantially increases this value by ~90 mV. In the case of five-membered rings (structure type C) the N effect is even more pronounced, leading to an OCP increase of ~100 mV (e.g. imidazole vs. pyrrole). The replacement of N by O in the five-

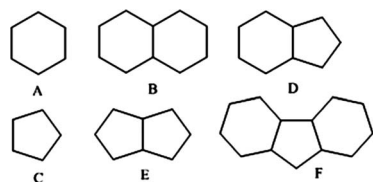


**Fig. 4** Structure types of potential organic carriers.

**Table 3** Hydrogen gravimetric densities and calculated open-circuit potentials for single six-membered (type A) and five-membered ring (type C) heterocyclic fuels

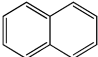
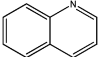
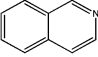
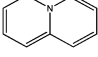
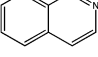
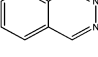
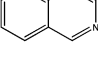
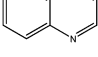
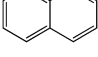
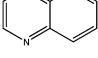
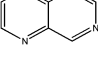
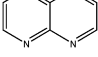
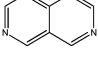
LOHC (in the dehydrogenated state)			
Name	Structure	H, wt%	$E^0$ , V
Benzene		7.19	1.049
Pyridine		7.10	1.081
Pyrimidine		7.02	1.116
Pyridazine		7.02	1.085
1,3,5-Triazine		6.94	1.198
Cyclopentadiene		5.75	0.854
Furan		5.59	1.004
1 <i>H</i> -Pyrrole		5.67	1.092
1 <i>H</i> -Imidazole		5.59	1.203
1 <i>H</i> -Pyrazole		5.59	1.269
1 <i>H</i> -1,2,3-Triazole		5.52	1.351
1 <i>H</i> -1,2,4-Triazole		5.52	1.328

membered ring is also quite significant since it decreases the OCP by ~90 mV (e.g. pyrrole vs. furan). Compounds with a single N–N bond (pyrazole, triazoles) have even higher OCP, exceeding that of the hydrogen fuel cell. However, due to possible hydrogenolysis of the N–N bond (much weaker than the C–C bond), this class of fuels might be unfit for the proposed fuel cell/flow battery system.

Table 4 shows the estimated OCPs for fused six-membered ring systems (structure type B). In type B structures, addition of one, two and even four nitrogen atoms does not substantially increase the OCP. Remarkably, the placement of the nitrogen atom in the ring does not play a significant role (compare isoquinoline and quinoline where the OCP change is about 20 mV). Only in the case of pyrimido[4,5-*d*]pyrimidine, with two pairs of 1,3-nitrogen atoms, the OCP could be raised higher by around ~88 mV when compared to the value of naphthalene.

The estimated OCPs for structure types D and E are shown in Table 5. Properties of these systems differ from systems having structure types A–C. For this type of structure the placement of a nitrogen atom in the five-membered ring affects the OCP (compare indole and isoindole), with the position in conjugation with the six-membered ring being the most beneficial. The

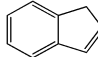
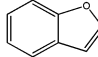
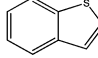
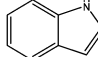
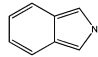
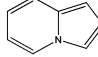
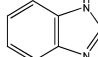
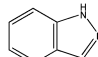
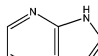
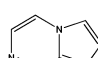
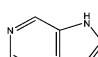
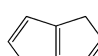
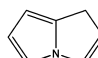
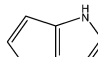
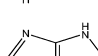
**Table 4** Hydrogen gravimetric densities and calculated open-circuit potentials for fused six-membered ring heterocyclic fuels (type B)

Organic carrier (in the dehydrogenated state)			
Name	Structure	H, wt%	$E^0$ , V
Naphthalene		7.29	1.078
Quinoline		7.24	1.097
Isoquinoline		7.24	1.098
4 <i>H</i> -Quinolizine		5.79	0.946
Cinnoline		7.19	1.087
Phthalazine		7.19	1.098
Quinazoline		7.19	1.119
Quinoxaline		7.19	1.108
1,8-Naphthyridine		7.19	1.112
1,5-Naphthyridine		7.19	1.115
Pteridine		7.09	1.128
Pyrazino[2,3- <i>b</i> ]pyrazine		7.09	1.122
Pyrimido[4,5- <i>d</i> ]pyrimidine		7.09	1.160

addition of a second nitrogen atom (*e.g.* in benzimidazole) makes the OCP close to that of the hydrogen fuel cell (50 mV difference). For purine, with two pairs of nitrogen atoms in the 1,3-position, the difference with the hydrogen fuel cell is even smaller with a potential of 1.228 V. However, the best result is found for structure type E with 1,3-nitrogen atoms where the potential is predicted to be 1.313 V.

The estimated OCPs for structure type F are shown in Table 6. This is the most interesting structure type, from a practical point of view, due to the high hydrogen content and proven reversibility of the thermal dehydrogenation reaction.<sup>22</sup> In this case the OCP for type F fuels with a substituent X in the 9th position increases in the order X = BH < CH<sub>2</sub> < S < O < NH, *i.e.* the opposite trend observed in the five-membered ring systems (type C). Addition of a nitrogen atom into each six-membered ring of carbazole increases the OCP by around 50 mV and reduces the difference with the hydrogen fuel cell to only 30 mV, in the case of the 1,8-diazacarbazole isomer. Replacement of a hydrogen atom at a non-aromatic nitrogen atom with an alkyl group (Me

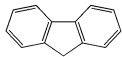
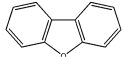
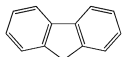
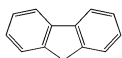
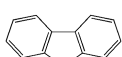
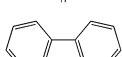
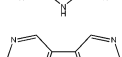
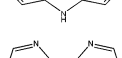
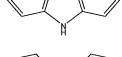
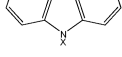
**Table 5** Hydrogen gravimetric densities and calculated open-circuit potentials for fused six- (type D) and five-membered (type E) ring heterocyclic fuels

Organic carrier (in the dehydrogenated state)			
Name	Structure	H, wt%	$E^0$ , V
1 <i>H</i> -Indene		6.49	1.041
Benzofuran		6.39	1.084
Benzo[ <i>b</i> ]thiophene		5.67	1.080
1 <i>H</i> -Indole		6.54	1.128
2 <i>H</i> -Isoindole		6.54	1.092
Indolizine		6.54	1.064
1 <i>H</i> -Benzo[ <i>d</i> ]imidazole		6.49	1.187
1 <i>H</i> -Indazole		6.49	1.206
1 <i>H</i> -Pyrrolo[2,3- <i>b</i> ]pyridine		6.39	1.167
Imidazo[1,2- <i>a</i> ]pyrazine		6.34	1.145
7 <i>H</i> -Purine		6.29	1.228
1,4-Dihydropentalene		5.49	0.901
1 <i>H</i> -Pyrrolizine		5.44	1.017
1,4-Dihydropyrrolo[3,2- <i>b</i> ]pyrrole		5.39	1.159
1,4-Dihydroimidazo[4,5- <i>d</i> ]imidazole		5.30	1.313

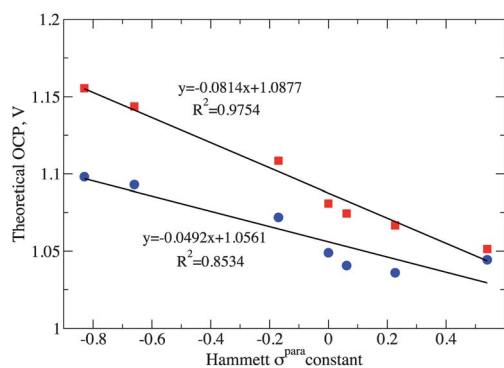
or Et) either does not change or even slightly increases (carbazole and diazacarbazole) the OCP. However, a promising result is found for the *N*-ethyl-1,8-diazacarbazole for which the predicted potential equals that of the hydrogen fuel cell.

Introduction of a donor group in the side chain of carbocyclic or heterocyclic saturated compounds increases the OCP. The effect is more pronounced (up to 70 mV for an amino-group) for *para*-substituted piperidines compared with substituted cyclohexanes (up to 40 mV), while electron-withdrawing groups decrease the OCP. In Fig. 5 we display the linear correlation between the OCP and the Hammett  $\sigma_{para}$  constants with better

**Table 6** Hydrogen gravimetric densities and calculated open-circuit voltages for fused six–five–six and five–five–membered ring heterocyclic fuels (type F)

Organic carrier (in the dehydrogenated state)			
Name	Structure	H, wt%	$E^0$ , V
9 <i>H</i> -Fluorene		6.78	1.109
Dibenzo[ <i>b,d</i> ]furan		6.71	1.125
Dibenzo[ <i>b,d</i> ]thiophene		6.16	1.117
5 <i>H</i> -Dibenzo[ <i>b,d</i> ]borole		6.81	1.108
9 <i>H</i> -Carbazole		6.75	1.152
9 <i>H</i> -Pyrrolo[2,3- <i>b</i> :5,4- <i>b'</i> ]dipyridine		6.67	1.206
5 <i>H</i> -Pyrrolo[3,2- <i>c</i> :4,5- <i>c'</i> ]dipyridine		6.67	1.191
5 <i>H</i> -Pyrrolo[3,2- <i>b</i> :4,5- <i>b'</i> ]dipyridine		6.67	1.181
9 <i>X</i> -Carbazole		H 6.75	1.152
		Et	1.167
9 <i>X</i> -1,8-diazacarbazole		H 6.67	1.206
		Me	1.222
		Et	1.230

$R^2$  for the piperidines. The hydroxyl group (not shown) is a clear outlier (the OCP is well below the predicted value), probably due to the formation of stabilizing hydrogen bonds not accounted for in the computation or formation of pyridine-4(1*H*)-one instead of 4-hydroxypyridine that increases OCP by about 30 mV.

**Fig. 5** Correlation of theoretical cell OCP with Hammett constants for fuels with substituents in the side chain of cyclohexane (blue dots) and piperidine (red dots).

## Conclusions

The established correlation between the OCPs obtained from experimental thermodynamic data and those calculated using DFT-based computational methods for molecules in the gas phase, allows for the assessment of a wide range of LOHCs for virtual hydrogen fuel cells. We find that both carbocyclic and N-heterocyclic analogues are good fuel candidates. From the analysed carbocyclic and heterocyclic organic compounds, nitrogen-containing fuels with fused five-membered rings are the more promising candidates, as assessed by the high OCPs and hydrogen content. Alkyl substitutional groups of cyclic fuel molecules allow for tuning the physical properties that determine the temperature range of the fuel liquid state (*e.g.*, the melting point) without significantly affecting the resulting OCPs.

It should be noted that the theoretical energy density of a fuel cell anode depends on the cell OCP and also on the hydrogen content and density of an organic carrier. The parameters discussed here indicate only the potential maximum specific energy stored/released and do not predict reaction kinetics – these lead to the presence of an overpotential and therefore must ultimately be considered along with the details of fuel cell design, such as compatibility of the fuel with the fuel cell PEM, to determine the practical energy density and efficiency.

## Acknowledgements

This material is based upon work supported as part of the Center for Electrocatalysis, Transport Phenomena, and Materials (CETM) for Innovative Energy Storage, an Energy Frontier Research Center funded by the U.S. Department of Energy, Office of Science, Office of Basic Energy Sciences under award number DE-SC00001055. V.S.B. acknowledges the allocation of computer time from NERSC. The authors thank Dr Matthew Rainka, Dr Andrea Peters (GE Global Research) for useful discussions and Mr James Presley, Dr Thomas Early, and Dr Maria LaTorre (GE Global Research) for help with experimental work. C.M.A. acknowledges a grant from Yale Climate and Energy Institute (YCEI).

## Notes and references

- G. L. Soloveichik, *Annu. Rev. Chem. Biomol. Eng.*, 2011, **2**, 503–527.
- T. Nguyen and R. F. Savinell, *Electrochem. Soc. Interface*, 2010, 54–56, Fall 2010.
- N. Armaroli and V. Balzani, *Energy Environ. Sci.*, 2011, **4**, 3193–3222.
- (a) D. U. Eberle and D. R. von Helmolt, *Energy Environ. Sci.*, 2010, **3**, 689–699; (b) U. Eberle, M. Felderhoff and F. Schüth, *Angew. Chem., Int. Ed.*, 2009, **48**, 6608–6630; (c) M. Biemann, U. F. Vogt, M. Zimmermann and A. Züttel, *J. Power Sources*, 2011, **196**, 4054–4060.
- (a) F. Crotogino, S. Donadei, U. Bunger and H. Landinger, *Large-Scale Hydrogen Underground Storage for Securing Future Energy Supplies*, Essen, Germany, May 16–21, 2010; (b) A. O. Converse, *Proc. IEEE*, 2012, **100**, 401–409.
- Praxair, Instantaneous hydrogen supply with cavern storage, <http://www.praxair.com/praxair.nsf/7a1106cc7ce1c54e85256a9c005accd7/3a0ab529a089b473852571f0006398a3!OpenDocument>.
- L. Hedström, M. S. Anders Folkesson, C. Wallmark, K. Haraldsson, M. Bryngelsson and P. Alvfors, *Bull. Sci. Tech. Soc.*, 2006, **26**, 264–277.
- (a) C. Weidenthaler and M. Felderhoff, *Energy Environ. Sci.*, 2011, **4**, 2495–2502; (b) J. Yang, A. Sudik, C. Wolverton and D. J. Siegel, *Chem. Soc. Rev.*, 2010, **39**, 656–675.



- 9 USDOE, Targets for onboard hydrogen storage systems for light-duty vehicles, [http://www1.eere.energy.gov/hydrogenandfuelcells/storage/pdfs/targets\\_onboard\\_hydro\\_storage\\_explanation.pdf](http://www1.eere.energy.gov/hydrogenandfuelcells/storage/pdfs/targets_onboard_hydro_storage_explanation.pdf).
- 10 (a) R. H. Crabtree, *Energy Environ. Sci.*, 2008, **1**, 134; (b) M. Ichikawa, in *Solid-State Hydrogen Storage: Materials and Chemistry*, ed. G. Walker, CRC Press, Boca Raton, 2008, ch. 18, pp. 500–532; (c) D. Teichmann, W. Arlt, P. Wasserscheid and R. Freymann, *Energy Environ. Sci.*, 2011, 2767–2773.
- 11 G. Cacciola, N. Giordano and G. Restuccia, *Int. J. Hydrogen Energy*, 1984, **9**, 411–419.
- 12 R. B. Biniwale, S. Rayalu, S. Devotta and M. Ichikawa, *Int. J. Hydrogen Energy*, 2008, **33**, 360–365.
- 13 G. L. Soloveichik and J. C. Zhao, *US Pat.*, App. 20080248345, 2008.
- 14 G. L. Soloveichik, J.-P. Lemmon and J. C. Zhao, *US Pat.*, App. 20080248339, 2008.
- 15 (a) N. Kariya, A. Fukuoka and M. Ichikawa, *Suiso Enerugi Shisutemu*, 2005, **30**, 91–94; (b) N. F. Kariya, A. Fukuoka and M. Ichikawa, *Phys. Chem. Chem. Phys.*, 2006, **8**, 1724–1730; (c) Y. Ando, T. Tanaka, T. Doi and T. Takashima, *Energy Convers. Manage.*, 2001, **42**, 1807–1816; (d) H. J. Kim, S. M. Choi, S. H. Nam, M. H. Seo and W. B. Kim, *Appl. Catal., A*, 2009, **352**, 145–151.
- 16 (a) Y. Ando, *J. Jpn. Inst. Energy*, 2004, **83**, 965–969; (b) Y. Ando, Y. Aoyama, T. Sasaki, Y. Saito, H. Hatori and T. Tanaka, *Bull. Chem. Soc. Jpn.*, 2004, **77**, 1855–1859; (c) K. Akimoto, *JP Pat. App.*, 2007287357, 2007.
- 17 Y. Cui, S. Kwok, A. Bucholtz, B. Davis, R. A. Whitney and P. G. Jessop, *New J. Chem.*, 2008, **32**, 1027–1037.
- 18 A. Moores, M. Poyatos, Y. Luo and R. H. Crabtree, *New J. Chem.*, 2006, **30**, 1675–1678.
- 19 G. B. DeLancey, S. Kovenklioglu, A. B. Ritter and J. C. Schneider, *Ind. Eng. Chem. Process Des. Dev.*, 1983, **22**, 639–645.
- 20 E. Newson, T. Haueter, P. Hottinger, F. Von Roth, G. W. H. Scherer and T. H. Schucan, *Int. J. Hydrogen Energy*, 1998, **23**, 905–909.
- 21 (a) N. Kariya, A. Fukuoka and M. Ichikawa, *Appl. Catal., A*, 2002, **233**, 91–102; (b) D. Sebastián, E. G. Bordejé, L. Calvillo, M. J. Lázaro and R. Moliner, *Int. J. Hydrogen Energy*, 2008, **33**, 1329–1334; (c) S. Hodoshima, H. Arai and Y. Saito, *Int. J. Hydrogen Energy*, 2003, **28**, 197–204.
- 22 G. P. Rez, A. R. Scott, A. C. Copper and H. Cheng, *US Pat.*, 7101530, 2006.
- 23 (a) G. P. Rez, A. R. Scott, A. C. Copper and H. Cheng, *US Pat.*, 7429372, 2008; (b) G. P. Rez, A. R. Scott, A. C. Copper, H. Cheng, F. C. Wilhelm and A. H. Abdourazak, *US Pat.*, 7351395, 2008.
- 24 (a) K. M. Eblagon, D. Rentsch, O. Friedrichs, A. Remhof, A. Zuetzel, A. J. Ramirez-Cuesta and S. C. Tsang, *Int. J. Hydrogen Energy*, 2010, **35**, 11609–11621; (b) K. M. Eblagon, K. Tam, K. M. K. Yu and S. C. E. Tsang, *J. Phys. Chem. C*, 2012, **116**, 7421–7429.
- 25 Z. Wang, I. Tonks, J. Belli and C. M. Jensen, *J. Organomet. Chem.*, 2009, **694**, 2854–2857.
- 26 F. Sotoodeh and K. J. Smith, *Ind. Eng. Chem. Res.*, 2010, **49**, 1018–1026.
- 27 H. Y. Zhao, S. T. Oyama and E. D. Naeemi, *Catal. Today*, 2010, **149**, 172–184.
- 28 E. S. Domalski and E. D. Hearing, *J. Phys. Chem. Ref. Data*, 1993, **22**, 805–1159.
- 29 (a) L. Glasser and H. D. B. Jenkins, *Thermochim. Acta*, 2004, **414**, 125–130; (b) L. Glasser and H. D. B. Jenkins, *Chem. Soc. Rev.*, 2005, **34**, 866–874.
- 30 A. Vatani, M. Mehrpooya and F. Gharagheizi, *Int. J. Mol. Sci.*, 2007, **8**, 407–432.
- 31 E. Clot, O. Eisenstein and R. H. Crabtree, *Chem. Commun.*, 2007, 2231–2233.
- 32 H. Dau, C. Limberg, T. Reier, M. Risch, S. Roggan and P. Strasser, *ChemCatChem*, 2010, **2**, 724–761.
- 33 J. Sefcik and W. A. Goddard Iii, *Geochim. Cosmochim. Acta*, 2001, **65**, 4435–4443.
- 34 (a) Wavefunction Inc., Irvine, CA, 2008; (b) W. J. Hehre and S. Ohlinger, *Spartan'08 for Windows, Macintosh and Linux User's Guide and Tutorial*, Wavefunction, Inc., Irvine, CA, 2008.
- 35 M. J. Frisch, G. W. Trucks, H. B. Schlegel, G. E. Scuseria, M. A. Robb, *et al.*, Gaussian 09, Revision A.1, Gaussian, Inc., Wallingford, CT, 2009.
- 36 (a) A. D. Becke, *Phys. Rev. A: At., Mol., Opt. Phys.*, 1988, **38**, 3098–3100; (b) C. Lee, W. Yang and R. G. Parr, *Phys. Rev. B: Condens. Matter Mater. Phys.*, 1988, **37**, 785–789; (c) A. D. Becke, *J. Phys. Chem.*, 1993, **98**, 5648–5652.
- 37 (a) J. T. H. Dunning, *J. Phys. Chem.*, 1989, **90**, 1007–1023; (b) R. A. Kendall, J. T. H. Dunning and R. J. Harrison, *J. Phys. Chem.*, 1992, **96**, 6796–6806; (c) D. E. Woon and J. T. H. Dunning, *J. Phys. Chem.*, 1994, **100**, 2975–2988.
- 38 NIST Standard Reference Database Number 69 Release edn., 2005.
- 39 S. A. Ali, in *Hydroprocessing of Heavy Oils and Residua*, ed. J. Ancheyta and J. G. Speight, CRC Press, 2007, pp. 51–69.
- 40 ASTM International, 2000.
- 41 (a) J. G. Liu, T. S. Zhao, R. Chen and C. W. Wong, *Electrochem. Commun.*, 2005, **7**, 288–294; (b) J. Ge and H. Liu, *J. Power Sources*, 2005, **142**, 56–69.
- 42 J. Mergel, A. Gluesen and C. Wannek, *Current Status of and Recent Developments in Direct Liquid Fuel Cells*, 2010.
- 43 EG&G Services Parsons, *Fuel Cell Handbook*, U.S. Department of Energy, Office of Fossil Energy, Morgantown, West Virginia, 2004.
- 44 W. S. Ohlinger, P. E. Klunzinger, B. J. Deppmeier and W. J. Hehre, *J. Phys. Chem. A*, 2009, **113**, 2165–2175.
- 45 F. Sotoodeh, L. Zhao and K. J. Smith, *Appl. Catal., A*, 2009, **362**, 155–162.